Medial Residues of Piecewise Linear Manifolds

Erin W. Chambers* Tao Ju† David Letscher‡

Abstract

Skeleton structures of objects are used in a wide variety of applications such as shape analysis and path planning. One of the most widely used skeletons is the medial axis, which is a thin structure centered within and homotopy equivalent to the object. However, on piecewise linear surfaces, which are one of the most common outputs from surface reconstruction algorithms, natural generalizations of typical medial axis definitions may fail to have these desirable properties. In this paper, we propose a new extension of the medial axis, called the medial residue, and prove that it is a finite curve network homotopy equivalent to the original surface when the input is a piecewise linear surface with boundary. We also develop an efficient algorithm to compute the medial residue on a triangulated mesh, building on previously known work to compute geodesic distances.

1 Introduction

The medial axis of an object is a skeletal structure originally defined by Blum [1]. It is the set of points having more than one closest points (under the Euclidean distance metric) on the boundary of the object. The medial axis is centered within the object, homology equivalent to the object if it is an open bounded subset of $\mathbb{R}^n$ [6], and (at least) one dimension lower than that of the object. These properties make the medial axis ideal for many applications including shape analysis and robotic path planning.

We are interested in defining a similar skeletal structure on a surface S (with boundary) that inherits the properties of the medial axis. Such a structure could then be used for applications such as shape analysis of surface patches as well as path planning in non-planar domains. We are particularly interested in the case when S is piecewise smooth, which is more representative of typical outputs of discrete surface reconstruction algorithms (e.g., triangulated meshes) than globally smooth surfaces.

*Department of Mathematics and Computer Science, Saint Louis University, echambe5@slu.edu. Research supported in part by NSF grant (CCF 1054779).

†Department of Computer Science and Engineering, Washington University in St. Louis, taoju@cse.wustl.edu. Research supported in part by NSF grant (IIS 0846072).

‡Department of Mathematics and Computer Science, Saint Louis University, letscher@slu.edu.

A natural approach would be to replace the Euclidean distances in the medial axis definition by geodesic distances over S [12]. Interestingly, as we will show in this paper (Section 3), several equivalent definitions of the medial axis may yield different structures when S is only piecewise smooth, and none of these definitions guarantees the two essential properties of the medial axis, namely being homotopy equivalent to the original surface and codimension one.

In this paper, we propose a new extension of the medial axis onto a piecewise linear surface S with boundary, which we call the *medial residue* (Section 4), and prove that the structure is a finite curve network that is always homotopy equivalent to S (Section 5). We also describe a quadratic-time algorithm to compute this structure on a piecewise flat surface with boundary embedded in Euclidean space (Section 6).

2 Background and Definitions

We assume the reader is familiar with classical definitions of manifold topology, which can be found in books such as [5, 9, 2]. We shall only review definitions that are specifically relevant to our work.

A *piecewise linear surface* is a 2-manifold (with boundary) with a piecewise linear structure, whose presentation consists of a finite number of triangles glued together along with an intrinsic distance metric on each triangle that is a linear map. Our algorithmic results work in a more restricted class of *piecewise flat surface*, where the piecewise linear structure comes from an embedding of a triangulation of M into $\mathbb{R}^3$, so that each triangle will be isometric to a triangle in $\mathbb{R}^2$.

Given a vertex v of a piecewise linear surface which is contained in more than two triangles, let $\{f_1, f_2, \ldots, f_k\}$ be the faces to which v belongs, where $\theta_i(v)$ is the interior angle of f_i at vertex v. The *total angle* is the sum of all of these angles, $\theta(p) = \sum_i \theta_I(v)$. The *curvature* at v is the value $2\pi - \theta(p)$. A vertex is said to be *convex*, *flat* or *concave* if its curvature is positive, zero or negative.

A *curve* (or path) is (the image of) a map $p : [0, 1] \to M$; the length of the curve is generally the length of the image in M. A curve is a *geodesic* if it is locally shortest; in other words, no perturbation of the curve will result in a shorter curve. On a piecewise linear surface, geodesics and shortest paths are themselves piecewise linear maps. We say a curve γ *bisects* a piecewise differentiable curve X at time t if $\gamma(t) \in X$ and the two

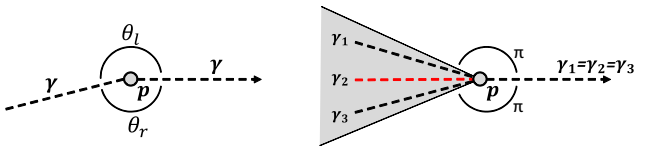

Figure 1: Left: Illustration of left and right curve angles. Right: at a concave vertex p, there may be infinitely many geodesic paths to the boundary (such as $\gamma_1, \gamma_2, \gamma_3$) sharing a common outgoing direction, but only one of them (γ_2) can be straight. Shaded region is the shadow rooted at p, made up of points whose shortest paths to the boundary go through p.

angles bounded by γ and the tangent of X at $\gamma(t)$ are equal. The *curve angles* θ_l and θ_r of a point p on a piecewise linear curve γ are the two angles to the left and right of the curve at p, where $\theta_l + \theta_r$ is the total vertex angle at that point p (see Figure 1 left).

A curve γ is considered *straight* if for each point $p \in \gamma$, the left and right curve angles are equal. This definition was introduced by Polthier and Schmies [10]. It is worth noting that Polthier and Schmies used the term "straight geodesic", and not simply straight. However, their straight geodesics might in fact not be geodesic (for example, it can go through a convex vertex). In this paper, the term straight geodesic will be used to denote a curve that is both straight and geodesic. Note that although there may be infinitely many geodesic paths to the boundary that go through a concave vertex p, only one of them is straight (see Figure 1 right). We call the region made up of points whose shortest paths to the boundary go through p the *shadow* rooted at p (shaded region in Figure 1 right).

3 The Medial Axis

Let X be a shape in Euclidean space. There are a variety of equivalent ways in which the medial axis of X could be defined. We will consider the following three:

1. Most commonly, the medial axis is defined as the set of points *without a unique closest point* on the boundary of the shape: $\mathcal{M}^{CP} = \{x \in X \mid \nexists \text{ unique } y \in \partial X \text{ with } d(x, \partial X) = d(x, y)\}$

2. Alternatively, the medial axis is the set of points *without a unique shortest path* to the boundary of the shape: $\mathcal{M}^{SP} = \{x \in X \mid \exists \text{ shortest paths } \gamma_1 \neq \gamma_2 \text{ from } x \text{ to } \partial X\}$

3. The medial axis is also the set of points *without a unique direction for shortest paths* to the boundary of the shape. We say two paths γ_1 and γ_2 with $\gamma_1(0) = \gamma_2(0)$ start in the same direction if there exists some $\epsilon > 0$ such that for all $t < \epsilon$, $\gamma_1(t) = \gamma_2(t)$ (or the curves can be reparameterized so that this holds): $\mathcal{M}^{SPD} = \{x \in X \mid \exists \text{ shortest paths } \gamma_1, \gamma_2 \text{ from } x \text{ to } \partial X \text{ that do not start in the same direction}\}$

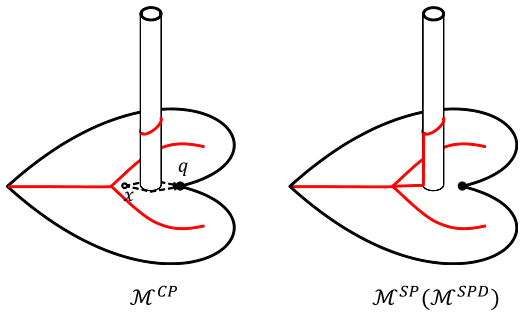

Figure 2: Example where $\mathcal{M}^{CP}$ (red) is not homotopy equivalent to the surface (but $\mathcal{M}^{SP}$ and $\mathcal{M}^{SPD}$ are).

We note that the above definitions are all equivalent when X is a smooth manifold in any dimension, but when X is piecewise smooth, these three definitions yield different structures. More precisely, if X is any path metric space (where distances are realized by shortest paths), then $M^{CP} \subset M^{SP}$ and $M^{SPD} \subset M^{SP}$. The fairly straightforward proof of this can be found in the full version of this paper. More importantly, there are situations where none of the three definitions satisfy the desired properties of being one dimension lower than and homotopy equivalent to X.

First, consider the heart-shaped surface in Figure 2, which has an interior hole on top of a cylindrical protrusion. Note that $\mathcal{M}^{CP}$ excludes points like x in the picture, which has a single closest point q on the boundary (a C^0 corner point) but two shortest paths to q that go around the cylinder. As a result, $\mathcal{M}^{CP}$ consists of two disconnected components. On the other hand, x is included in $\mathcal{M}^{SP}$ and $\mathcal{M}^{SPD}$.

Next, consider the oval-shaped surface in Figure 3 (a). The surface has a concave vertex v with a large negative curvature that happens to have two shortest paths to two distinct boundary points (a non-generic situation). Since each point in the shadow rooted at v (shaded region in (b)) would have two distinct shortest paths to the boundary, both $\mathcal{M}^{CP}$ and $\mathcal{M}^{SP}$ include the 2-dimensional shadow region. On the other hand, since any point in the shadow has a unique shortest path direction (that follows the geodesic to v), the entire shadow is excluded in $\mathcal{M}^{SPD}$, and $\mathcal{M}^{SPD}$ has an isolated vertex v that is disconnected from the rest of $\mathcal{M}^{SPD}$.

4 The Medial Residue

We now define our structure, called the medial residue, which is equivalent to existing definitions of the medial

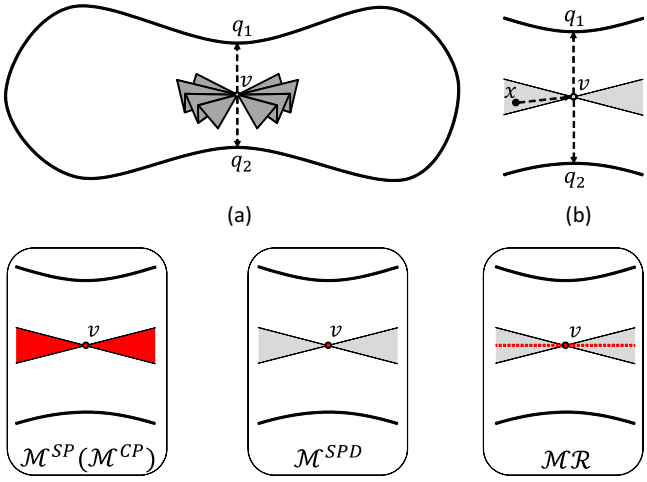

Figure 3: Top: a surface with a highly concave central vertex (a) and a zoom-in view (b). Bottom: different medial axis extensions (red): $\mathcal{M}^{CP}$ and $\mathcal{M}^{SP}$ are 2-dimensional, $\mathcal{M}^{SPD}$ has an isolated vertex, and $\mathcal{MR}$ is 1-dimensional and homotopy equivalent to the surface.

axis on a smooth manifold but possesses the desired properties of homotopy equivalence and co-dimension one on a piecewise linear surface. To make it clear that we are considering surfaces and not arbitrary manifolds from now on, we will use S instead of X to represent the shape.

We note that our medial residue is well defined on piecewise smooth manifolds, and that the majority of our results hold in these settings. However, our proof about homotopy and dimension holds only for piecewise linear surfaces, although we conjecture that the properties hold in more general settings as well.

The starting point of our definition is $\mathcal{M}^{SPD}$, which is more complete than $\mathcal{M}^{CP}$ in our first example (Figure 2) and remains low dimension in the second example (Figure 3). Our goal is to add low-dimensional components to $\mathcal{M}^{SPD}$ to restore the homotopy equivalence. Observe that, in our second example, the disconnection in $\mathcal{M}^{SPD}$ takes place in the shadow rooted at a concave vertex $v \in \mathcal{M}^{SPD}$, where the shortest paths from a point x in the shadow to the boundary would agree for some time and then diverge at v. Since we cannot include the entire shadow, which is 2-dimensional, we wish to keep one representative curve. A natural choice of such curve would be one that is "centered" with respect to the two diverging shortest paths at v. More precisely,

Definition 1 *The* medial residue, $\mathcal{MR}$ *consists of any point $x \in S$ such that either $x \in \mathcal{M}^{SPD}$ or where there are two distinct shortest paths from x to the boundary, γ_1 and γ_2, parameterized by arc length, which first intersect $\mathcal{M}^{SPD}$ at $v = \gamma_1(t) = \gamma_2(t)$ such that $\gamma = \gamma_1([0,t]) = \gamma_2([0,t])$ is straight and bisects the angle between the tangents of the two shortest paths from v to the boundary that are nearest to γ on its left and right side.*

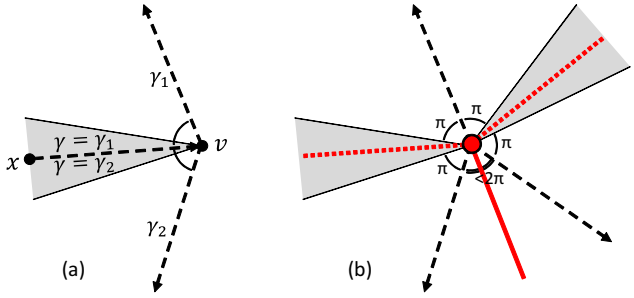

Figure 4: (a): illustration for the definition of a point $x \in \mathcal{MR} \setminus \mathcal{M}^{SPD}$. (b): a generic picture of $\mathcal{MR}$ at a concave vertex with multiple shortest path directions (solid line is $\mathcal{M}^{SPD}$ and dotted lines are $\mathcal{MR} \setminus \mathcal{M}^{SPD}$).

The definition for a point $x \in \mathcal{MR} \setminus \mathcal{M}^{SPD}$ is illustrated in Figure 4 (a). Note that, by definition, every point on the common segment γ of the shortest paths from x to the boundary is also included in $\mathcal{MR} \setminus \mathcal{M}^{SPD}$. In fact, $\mathcal{MR} \setminus \mathcal{M}^{SPD}$ consists of straight geodesics that bisect shortest path directions at concave vertices of $\mathcal{M}^{SPD}$. Figure 4 (b) gives a generic picture of $\mathcal{MR}$ at a concave vertex of $\mathcal{M}^{SPD}$. The multiple shortest path directions divide the local neighborhood of the vertex radially into *sectors*. Each sector is bisected either by a curve in $\mathcal{M}^{SPD}$ (solid red line), if the sector's interior angle is less than 2π, or otherwise by a curve in $\mathcal{MR} \setminus \mathcal{M}^{SPD}$ (dotted red line).

Since any point in $\mathcal{MR} \setminus \mathcal{M}^{SPD}$ has two distinct shortest paths, we have $\mathcal{M}^{SPD} \subset \mathcal{MR} \subset \mathcal{M}^{SP}$. Since both $\mathcal{M}^{SPD}$ and $\mathcal{M}^{SP}$ are equivalent when S is a smooth manifold, this implies that our medial residue is also equivalent to the other definitions we mentioned earlier in a smooth manifold.

5 Medial Residue on Piecewise Linear Surfaces

In this section, we give sketches of proofs of Theorem 2 and the related lemmas, showing that the medial residue is homotopy equivalent to the original surface; full proofs of each appear in the full version of this paper. As previously mentioned, while we only prove this for piecewise linear surfaces (the main focus of this work), we conjecture that it also holds for piecewise smooth surfaces and higher dimensional manifolds as well.

Theorem 2 *If S is a piecewise linear surface with boundary then the medial residue of S is a finite graph that is a deformation retract of S.*

To prove this theorem, we will construct a deformation retract by incrementally "eroding" from the boundary, stopping at potentially interesting points along the way. To begin this process, we must understand what a neighborhood of the boundary of S looks like. Let $S_t = \{x \in S \mid d(x, \partial S) \geq t\}$; in other words, S_t is the set of points whose distance from the boundary of S is no less than t. The boundary of S_t is precisely the points with distance t to ∂S.

Our first step is to prove that shortest paths to the boundary are of finite complexity; in other words, they cannot cross the triangulation an unbounded number of times. If our PL surface is a flat embedding in $\mathbb{R}^3$, this will follow easily since edges in the triangulation are shortest paths (and no two shortest paths can cross twice), but we must also have a bound for arbitrary PL surfaces. We note that variants of the following proof have been used in the normal surface community for at least 20 years; however, we are unaware of any published reference for such a bound on the number of possible intersections, so we have included it for completeness.

Proposition 3 *The number of intersections between any shortest paths and the underlying triangulation of an arbitrary PL-surface is* $\leq |E| \cdot \frac{2\pi}{\delta} \cdot \max_{e \in E} \frac{l(e)}{c_e}$, *where* δ *is the minimum angle at any vertex of the triangulation,* $l(e)$ *is the length of the edge* e, *and* $c(e)$ *is the minimum distance between any pair of points on opposite edges of the quadrilateral formed by the two faces adjacent to an edge* e.

Next, we want to understand what the boundary of the surface looks like at each stage of the erosion process. Locally, ∂S_t consists of a union of straight edges and circular arcs. The straight edges correspond to points whose shortest paths to the boundary do not pass through a vertex of the triangulation, and the circular arcs to points whose shortest paths pass through a vertex. The previous proposition can be used to show that there are finitely many arcs and lines segments in ∂S_t.

Lemma 4 *Given a piecewise linear* S, *for all but finitely many values of* t, ∂S_t *is a curve. In the cases where* ∂S_t *is not a curve,* ∂S_t *is a graph.*

Notice that $\mathcal{M}^{SPD}$ consists of points that have multiple shortest paths directions to the boundary. The above results allow us to bound the combinatorial types of these shortest paths. The points equidistant from the boundary in each shortest path direction are built locally from lines segments and circular arcs. So in a small neighborhood $\mathcal{M}^{SPD}$ consists of the intersection of two curves that are either lines or circles. Hence, $\mathcal{M}^{SPD}$ is built from lines, circles and parabolas. This leads to the following result:

Lemma 5 *If* S *is piecewise linear, then* $\mathcal{M}^{SPD}$ *is a finite graph.*

Now we are ready to describe the deformation retract, which immediately implies that $\mathcal{MR}$ is homotopy equivalent to the original PL surface. We will build our deformation retract based on an erosion process which intuitively "pauses" at times $\{t_1, \ldots, t_k\}$, where each t_i corresponds to one or more of these three possibilities:

1. There is a vertex v of the triangulation of S with $d(v, \partial S) = t_i$.
2. ∂S_{t_i} is not a disjoint union of curves but instead forms a graph.
3. There is a vertex v of $\mathcal{M}^{SPD}$ with $d(v, \partial S) = t_i$.

The previous lemmas imply that the set of t_i's is finite. We will consider the sets S_{t_i} based on our level sets at times $\{t_1, \ldots, t_k\}$ described above, as well as the "slice" between two of our level sets, $C_i = \overline{(S_{t_i} \setminus S_{t_{i+1}})}$. The following lemma actually shows how we can construct the deformation retract.

Lemma 6 *For each* t_i, $S_{t_{i+1}} \cup \mathcal{MR}$ *is a deformation retract of* $S_{t_i} \cup \mathcal{MR}$.

Proof. Consider the slice region C_i between two level curves. One of several cases could occur depending on what happens on the boundaries of this region, as illustrated in Figure 5.

The first case is that portions of the boundary ∂S_{t_i} meet at a convex corner. This is shown in Figure 5(a), where the shortest paths are shown on the left and the deformation retract on the right. At such a corner point v, there is a segment of $\mathcal{M}^{SPD}$ going from ∂S_{t_i} to $\partial S_{t_{i+1}}$, which bisects the convex corner at v. Shortest paths from points on this segment hit ∂S_{t_i} near v. The deformation retract follows these curves.

The second case is that portions of the boundary ∂S_{t_i} meet at a concave corner, see Figure 5(b). Note that the concave corner v must contain a shadow rooted at v where there is a cone of shortest paths going through v. By definition of $\mathcal{MR}$, if $v \in \mathcal{MR}$ then the bisector of the shadow will be in $\mathcal{MR} \setminus \mathcal{M}^{SPD}$. However, the deformation retract cannot simply follow the shortest paths exactly, as this would not be continuous at v; observe in the figure that points near v are taken to opposite sides of the bisector and do not move continuously. Instead, very near this point, the deformation retract will take points to either the bisector or the full shadow, as shown on the right in Figure 5(b). Note that the reparameterization continuously deforms points from ∂S_{t_i} onto the union of $\partial S_{t_{i+1}}$ and $\mathcal{MR}$.

In the third case, consider points $v \in \partial S_{t_i}$ where the ∂S_{t_i} is smooth. A single shortest path passes through v. If $v \notin \mathcal{MR}$, the deformation retract simply follows this path backwards, as shown in Figure 5(c). Otherwise, if $v \in \mathcal{MR}$, there is a segment of a bisector in $\mathcal{MR}$ that contains v and continues in a direction that

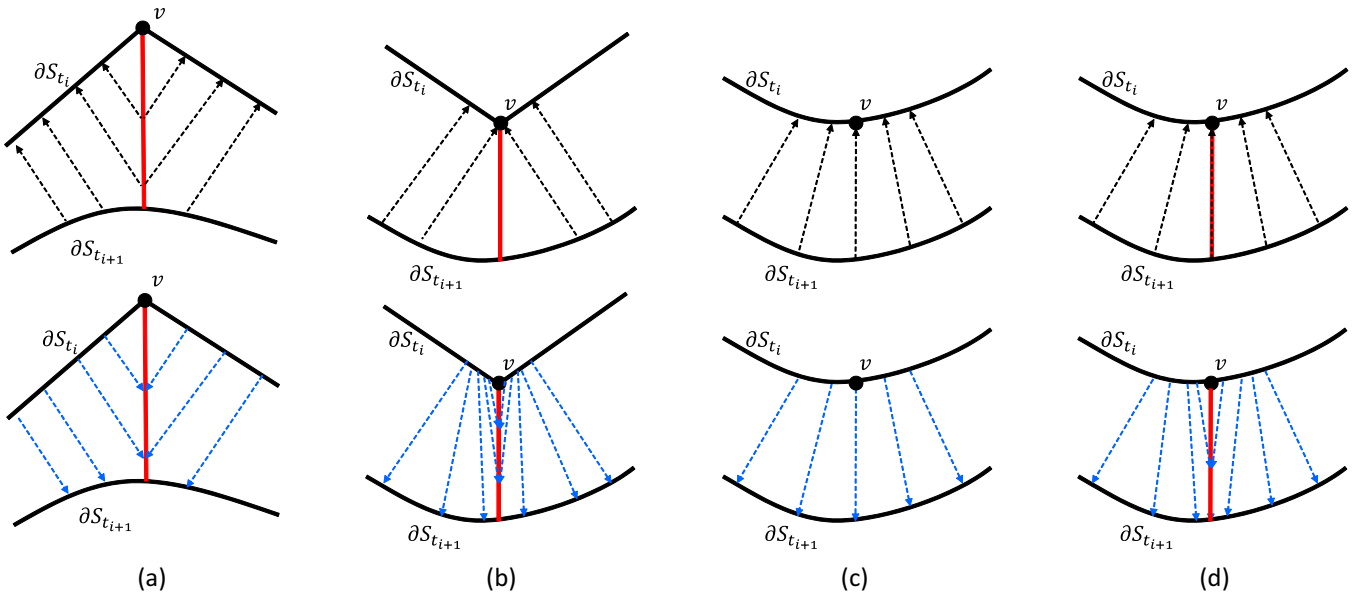

Figure 5: The shortest paths (black arrows), medial residue (red lines) and deformation retract (blue arrows) at the points in the slice region.

is perpendicular to ∂S_{t_i}. In this situation (as in the second case above), the shortest paths cannot be used as a deformation retract as it would not be continuous at that v. However, a similar re-parameterization as in the second case can be used in a local neighborhood of this portion of $\mathcal{MR}$ to construct a deformation retract, as shown in Figure 5(d).

Note that it is possible that ∂S_{t_i} is a graph, in which case the deformation retract described in the three cases above can be applied to individual components of C_i that are incident to a point $v \in \partial S_{t_i}$.

□

Finally, to show that $\mathcal{MR}$ is a finite graph, we observe that the set of concave vertices in $\mathcal{M}^{SPD}$ and the set of sectors around each such vertex are both finite on a PL surface, which implies that $\mathcal{MR} \setminus \mathcal{M}^{SPD}$ consists of a finite number of straight geodesic paths that bisect these sectors. Together with our previous lemma that $\mathcal{M}^{SPD}$ is a finite graph, this completes the proof of Theorem 2.

6 Algorithm

We next give an overview of our algorithm to compute the medial residue on a piecewise flat surface with triangle faces in $\mathbb{R}^3$, a commonly used discretization in many applications. (Further details of the algorithm can be found in the full version of the paper.)

We first recall some essential properties of shortest paths on a triangulated surface S [7, 4]. We assume the boundary ∂S consists of vertices and edges of some triangle faces. A shortest path p that connects any point $x \in S$ to the boundary ∂S originates either from a vertex or an interior point of an edge. In the latter case, p is orthogonal to that originating edge. The path p may go through some vertex of S, and if it does, both the left and right curve angles made by p at that vertex are greater than or equal to π. Away from the vertices, p is a straight line segment after unfolding the triangles that p goes through onto a plane. We call the last vertex visited by p before reaching x the *root* of p. If p does not go through any vertex, the root is the originating vertex or edge on ∂S. The *last edge sequence* of p is the (possibly empty) sequence of edges that p goes through between the root and x.

The starting point of our algorithm is a subdivision of each triangle face into regions where the shortest paths have a common combinatorial structure. Given a face f, a root r (being either a vertex or edge), and an edge sequence E, a *cell* is the set of points $x \in f$ such that some shortest path from x to ∂S has root r and last edge sequence E. The curve segments that bound the cells (including both interior segments on f and the segments on the edges of f) form a graph, which is called the *subdivision graph*. The subdivision can computed using an easy extension of existing methods [8, 7, 4] in $O(n^2 \log n)$ time and $O(n^2)$ space.

Given the subdivision graph, our algorithm first identifies a subset of the graph as $\mathcal{M}^{SPD}$, then adds in the bisectors to form the complete $\mathcal{MR}$. Both steps can be done in $O(n^2)$ time and space, where n is the number of triangles of the surface. The overall process, taking into account the creation of the face subdivision, can be

done in $O(n^2 \log n)$ time and $O(n^2)$ space. We assume exact arithmetic is used to precisely compute distances and angles.

6.1 Computing $\mathcal{M}^{SPD}$

First, we observe two relations between $\mathcal{M}^{SPD}$ and a subdivision graph:

Lemma 7 *$\mathcal{M}^{SPD}$ is a subset of the subdivision graph.*

Lemma 8 *Let h be a segment in the subdivision graph, then either all interior points of h lie in $\mathcal{M}^{SPD}$ or none of them does.*

The algorithm simply goes through each element (a vertex or a segment open at its ends) of the subdivision graph. For each element l, it picks an arbitrary point $x \in l$ and gathers shortest path directions at x by examining each incident cell of l. l is included in $\mathcal{M}^{SPD}$ as soon as two distinct shortest path directions are found.

Since computing the shortest path direction given a cell takes constant time, the complexity of the algorithm is proportional to the number of pairs of an element and an incident cell, which is linear to the number of elements in the subdivision graph. The algorithm uses a data structure that maintains adjacency between cells and subdivision graph elements, which is again linear to the complexity of the graph. Hence computing $\mathcal{M}^{SPD}$ can be done in $O(n^2)$ time and $O(n^2)$ space.

6.2 Computing $\mathcal{MR} \setminus \mathcal{M}^{SPD}$

We use a tracing algorithm to compute bisectors that make up $\mathcal{MR} \setminus \mathcal{M}^{SPD}$. For each sector bounded by shortest path directions at some concave vertex $v \in \mathcal{M}^{SPD}$, we start tracing a straight and shortest path from v in the bisecting direction of the sector. Tracing proceeds in a cell-by-cell manner, creating straight line segments within each cell and maintaining straightness while marching to the next cell. Tracing ends when the path hits a segment or vertex of the subdivision graph that belongs to $\mathcal{M}^{SPD}$.

Tracing within a cell involves intersecting a line with several low-degree algebraic curves. Since the intersection of a cell with a shortest path to the boundary is a single line segment [8], tracing in a cell can be done in time linear to the number of segments of the cell. Marching from one cell to the next can be done in constant time using an adjacency structure. To bound the complexity of tracing all bisectors, the key is to observe that each cell can contain a non-trivial portion of at most one bisector. This is because only a cell whose shortest paths to the boundary are rooted at some vertex may contain a bisector rooted at the vertex, and the angle made by any two bisectors rooted at a vertex is at least 2π. So the total tracing time for all bisectors is bounded by the sum of number of segments over all cells, which is $O(n^2)$. Tracing uses $O(n^2)$ space since it adds only a constant amount of additional data per element of the subdivision graph.

References

[1] H. Blum. A transformation for extracting new descriptors of form. *Models for the Perception of Speech and Visual Form*, pages 362–80, 1967.

[2] Manfredo P. Do Carmo. *Differential Geometry of Curves and Surfaces*. Prentice Hall, 1976.

[3] Jeff Erickson and Amir Nayyeri. Tracing compressed curves in triangulated surfaces. In *Proceedings of the 2012 symposuim on Computational Geometry*, SoCG '12, pages 131–140, New York, NY, USA, 2012. ACM.

[4] M. Fort and J.A. Sellares. Generalized source shortest paths on polyhedral surfaces. In *Proceedings of the 23rd European Workshop on Computational Geometry*, pages 186–189, March 2007.

[5] Allen Hatcher. *Algebraic Topology*. Cambridge University Press, 2002.

[6] André Lieutier. Any open bounded subset of $\mathbb{R}^n$ has the same homotopy type as its medial axis. *Computer-Aided Design*, 36(11):1029 – 1046, 2004. Solid Modeling Theory and Applications.

[7] Joseph S. B. Mitchell, David M. Mount, and Christos H. Papadimitriou. The discrete geodesic problem. *SIAM J. Comput.*, 16(4):647–668, August 1987.

[8] David Mount. Voronoi diagrams on the surface of a polyhedron. Technical report, Dept. of Computer Science, Univ. of Maryland, Baltimore, MD, 1985.

[9] James Munkres. *Topology*. Pearson, 2000.

[10] Konrad Polthier and Markus Schmies. Straightest geodesics on polyhedral surfaces. In *ACM SIGGRAPH 2006 Courses*, SIGGRAPH '06, pages 30–38, New York, NY, USA, 2006. ACM.

[11] Micha Sharir. Intersection and closest-pair problems for a set of planar discs. *SIAM J. Comput.*, 14(2):448–468, 1985.

[12] F.-E. Wolter and K.-I. Friese. Local and global geometric methods for analysis interrogation, reconstruction, modification and design of shape. In *Proceedings of the International Conference on Computer Graphics*, CGI '00, pages 137–151, Washington, DC, USA, 2000. IEEE Computer Society.